

Density fluctuations in the intermediate glass-former glycerol: a Brillouin light scattering study

Lucia Comez, Daniele Fioretto, Filippo Scarponi

Dipartimento di Fisica and INFM, Università di Perugia, I-06123, Perugia, Italy.

Giulio Monaco

European Synchrotron Radiation Facility, B.P. 220 F-38043, Grenoble, France.

Brillouin scattering has been used to measure the dynamic structure factor of glycerol as a function of temperature from the high temperature liquid to the glassy state. Our investigation aims at understanding the number and the nature of the relaxation processes active in this prototype glass forming system in the high frequency region. The associated character of glycerol is reflected by a rather simple relaxations pattern, while the contributions coming from intra-molecular channels are negligible in the GHz frequency region. The temperature behavior of the characteristic frequency and lifetime of the longitudinal acoustic modes is analyzed, suggesting that a phenomenological model which only includes the structural (α) process and the unrelaxed viscosity is able to catch the leading contributions to the dynamics of the density fluctuations. This ansatz is also supported by a combined analysis of light and inelastic x-ray scattering spectra. The temperature dependence of the characteristic time of the α -process, τ_α , obtained by a full-spectrum analysis conforms to the α -scale universality, i.e. the values τ_α revealed by different experimental techniques are proportional the ones to the others. The non-ergodicity parameter smoothly decreases on increasing the temperature, and no signature of the cusp-like behavior predicted by the idealized mode coupling theory and observed in other glass-formers is found in glycerol.

I. INTRODUCTION

Density fluctuations hold a key role in the dynamics of glass-forming systems: the glass formation itself is related to the progressive arrest of long time density fluctuations. The characteristic time τ_α of these fluctuations exhibits a steep increase for temperatures approaching the glass transition temperature, T_g , ranging from $\sim 10^{-12}$ s well above the melting point to $\sim 10^2$ s at T_g . For this reason more than one technique is usually required to cover the whole time or frequency range where this dynamics takes place. Inelastic neutron, x-ray and light scattering are the experimental techniques most widely used to study the density fluctuations in supercooled systems. Among these, Brillouin light scattering (BLS) is a powerful tool to gain access to the spectrum of density fluctuations in the GHz region.

In the earliest BLS studies of glass forming systems, the data analysis was focused on measuring the frequency shift and linewidth of the Brillouin peaks, i.e. the phase velocity and absorption of the longitudinal acoustic modes [1, 2, 3]. The analysis of the temperature dependence of these parameters was used to determine either the temperature dependence of the relaxation time (activation plot) once the shape of the relaxation function was fixed, or, conversely, the shape of the structural relaxation (master plot) once the $\tau(T)$ behavior was given [4].

More recently, the improvements of interferometric setups allowed the experimentalists to obtain high-contrast and high-resolution BLS spectra in a wider frequency window ranging from few hundreds of MHz to few tens of GHz, thus gaining information on the shape of both the Brillouin peaks and the quasi-elastic central region

known as Mountain peak [5]. Thanks to these advances, it has become possible to carry out full spectrum analyses in a window of $1 \div 2$ decades in frequency, using expressions for the spectrum of density fluctuations derived within the Generalized Hydrodynamics formalism [6] or, equivalently, from a generalized Langevin equation [7]. The spectrum is thus written in terms of static correlators and of a frequency-dependent longitudinal modulus or, equivalently, longitudinal viscosity. In the earliest investigations of supercooled systems, reasonable fits of the measured spectra were obtained considering the α -relaxation as the only relevant relaxational process. In those investigations, the α -relaxation was typically described by the Cole-Davidson (CD) expression, like in the case of salol [8], PC [9], ZnCl_2 [10, 11]. The main limit of this approach is to ignore the possible presence of additional processes in the BLS frequency range, faster than the CD relaxation.

A contribution to the fast dynamics of density fluctuations in supercooled systems is predicted by the mode coupling theory (MCT) [12] as the fast component of the structural relaxation, also known as the mode coupling β region. During the last decade an important contribution to the comparison of the MCT predictions to Brillouin spectra has been given by Cummins and coworkers [13]. Another important contribution to the fast dynamics of density fluctuations in molecular liquids comes from internal thermal relaxations [14]. These are connected to the exchange of energy between acoustic waves and intramolecular degrees of freedom, like vibrations and rotations of groups of atoms. It is interesting to notice that the Generalized Hydrodynamic approach to Brillouin scattering was originally introduced in the sixties by Mountain and Zwanzig [5, 15] to explain exactly the

thermal relaxation in Kneser-type liquids [14], although its importance has been largely underestimated in more recent studies of supercooled systems. A clear signature of the existence of this relaxation channel in BLS spectra can be found in the almost Arrhenius temperature dependence of the relaxation time obtained by the single-relaxation analysis of different glass forming systems, both simple [9] and polymeric (see for instance, [16, 17]) in nature.

The main reason why a two-relaxation (α +thermal) model was not employed for long time in the analysis of BLS spectra can be found in the narrowness of the frequency window available to this technique. A step forward in the solution of this problem has been recently proposed, based on the combined use of ultrasonic, BLS and inelastic x-ray scattering (IXS) spectra. IXS is a novel technique which directly probes density fluctuations in the high q limit of some nm^{-1} , extending the frequency range accessible to Brillouin scattering investigations to the THz region. It is then now possible to carry out a full spectrum analysis in a reasonably wide spectral region, including both structural, thermal and unrelaxed viscosity ("instantaneous") processes. Using this method in polybutadiene [18] it was possible to separate the contribution of the α relaxation from that of the fast intramolecular process, and to reconcile the positive tests of MCT previously obtained by neutron scattering with BLS results. In ortho-terphenyl, the presence of a vibrational relaxation [19, 20] has been confirmed by BLS measurements on the single crystal [21], and by molecular dynamics simulations [22].

In this work, we study the high frequency dynamics of the glass former glycerol, an associated liquid which forms a H-bond network, making it intermediate between fragile and strong systems. Different from Kneser liquids, in associated liquids the ratio between the acoustic absorption α and the classical absorption α_{cl} (only due to shear viscosity and thermal conductivity) is very small (typically less than 3) and temperature independent. This feature is traditionally attributed to a negligible coupling of the acoustic waves with internal degrees of freedom. This simple relaxation pattern suggests glycerol as a natural candidate for testing glass formation theories.

Glycerol has already been the object of several studies concerning its acoustic properties and dynamical processes. Ultrasonic (US) measurements in the MHz frequency region have been reported of the adiabatic speed and of the absorption of sound [14, 23, 24, 25]. Photon correlation spectroscopy (PCS) has been used to characterize the structural relaxation close to T_g [26, 27]. Impulsive stimulated Brillouin and thermal light scattering (ISBS and ISTS) experiments [28, 29] have provided information on the sound dispersion and absorption and on the structural relaxation at low temperatures and for different q values. Stimulated Brillouin gain (SBG) spectroscopy has been also used to probe the dynamics of supercooled and glassy glycerol [30]. Very recently, the

density response of supercooled glycerol to an impulsive stimulated thermal grating has been studied in the 200-340 K temperature range in order to separate the structural relaxation from thermal diffusion processes [31]. Rayleigh-Brillouin spectra at very high resolution have been presented [32] to reveal acoustic anomalies in glassy glycerol at low temperatures. The temperature behavior of the structural relaxation process has also been studied by depolarized light and neutron scattering [33, 34, 35], and dielectric spectroscopy [36, 37, 38]. Moreover, inelastic x-ray scattering [39, 40, 41] has been used to investigate the high-frequency dynamics of supercooled glycerol and the nature of the acoustic attenuation at low temperatures. Despite of this extensive literature, there is no light scattering investigation which covers the entire range comprised between the high temperature liquid and the glassy state.

Here we report high resolution Brillouin spectra covering nearly two decades in frequency in a wide temperature range from 47 to 441 K. The main purpose of this paper is to contribute to the identification of the relaxation processes active in the GHz frequency region of glycerol, and to the characterization of their temperature evolution. In order to constrain the hydrodynamic model proposed for the density fluctuations, we perform a combined light and inelastic x-ray analysis. Moreover, a comparison is also reported with the results obtained by different techniques, including ISTS, ISBS, SBG, dielectric spectroscopy, photon correlation spectroscopy, and depolarized light scattering, in order to test the degree of universality of the temperature dependence of the characteristic time and of the shape parameters of the α relaxation.

Finally, a preliminary comparison with the predictions of the mode coupling theory of supercooled liquids is presented. MCT [12], considered the first microscopic model of the glass transition, describes the slowing down of the structural dynamics in terms of a non-linear coupling between density fluctuations which, if we neglect hopping processes, causes the structural arrest of the system at the critical temperature, T_c . Several studies have been previously performed to test the MCT predictions on glycerol. Depolarized light scattering [33, 34, 35] and neutron [33] and dielectric [36, 37, 38, 42] data have been subjected to MCT checks. All together these studies provide a variegated picture of the existence and the eventual location of the critical temperature, T_c : the different T_c evaluations span a range comprised between 250 and 310 K [33, 34, 35, 36, 37, 38, 42].

One of the main predictions of the idealized mode coupling theory concerns the temperature behavior of the non-ergodicity factor f_q — the normalized amplitude of the structural relaxation — which should exhibit a cusp at T_c . In this paper, by measuring the limiting low and high frequency adiabatic sound velocity in a wide temperature range, we derive the non-ergodicity factor [43] for the density fluctuations, and look for the possible existence of the crossover temperature predicted by MCT.

II. THEORETICAL BACKGROUND

A. Dynamic structure factor

An expression for the dynamic structure factor, and thus for isotropic Brillouin spectrum which is proportional to it, can be derived from the equation of motion of the microscopic density $\rho(r, t)$. In the limit of low thermal conductivity, density fluctuations are decoupled from temperature fluctuations, and the equation of motion of the q -th component of the microscopic density, $\rho(q, t)$, is derived within simple hydrodynamics and comes out to be that of a damped harmonic oscillator (DHO):

$$\left[\left(\frac{\rho_M}{q^2} \right) \frac{\partial^2}{\partial t^2} + \eta_L \frac{\partial}{\partial t} + M \right] \rho(q, t) = 0 \quad (1)$$

where ρ_M is the average mass density, η_L the longitudinal viscosity and M the longitudinal elastic modulus. The dynamic structure factor, $S(q, \omega)$, obtained from the Laplace-Fourier transform of Eq. (1), is:

$$S(q, \omega) = \frac{S(q)M}{\pi\omega} \frac{\omega\eta_L}{[\omega^2\rho_M/q^2 - M]^2 + [\omega\eta_L]^2}, \quad (2)$$

where $S(q)$ is the static structure factor. A Brillouin peak in the spectrum is thus expected close to

$$\omega_{LA} = q(M/\rho_M)^{1/2}, \quad (3)$$

proportional to the longitudinal acoustic (LA) velocity $c_{LA} = \omega_{LA}/q$. The full width of the peak

$$\Gamma_{LA} = q^2\eta_L/\rho_M \quad (4)$$

is proportional to the attenuation of the LA mode. In fact, the absorption of longitudinal acoustic modes is given by $\alpha = \Gamma_{LA}/2c_{LA}$. The integrated area of the spectrum is proportional to the adiabatic compressibility χ_S . In the limit of low thermal conductivity here considered, thermal fluctuations contribute only to the low frequency region of the spectrum, giving rise to the Rayleigh peak centered at frequency zero and linewidth of about 0.1 GHz. The total intensity, taking into account also this last contribution, is proportional to the isothermal compressibility χ_T . The ratio of the intensity of the Rayleigh line over the Brillouin lines $(\chi_T - \chi_S)/\chi_S = \gamma - 1 = R_{LP}$ is known as Landau-Placzek ratio.

In molecular liquids the acoustic modes may couple both with the molecular internal degrees of freedom and with the α process, giving rise to additional mechanisms of acoustic damping. These relaxation effects are also responsible for a peak at zero-frequency (Mountain peak) and can be taken into account by a generalization of the hydrodynamic equations, introducing an ω -dependent

modulus (or viscosity). In particular, the complex frequency dependent modulus $M(\omega) = M'(\omega) - iM''(\omega)$ can be written as:

$$M(\omega) = M_\infty + \Delta M(\omega) + i\omega\eta_\infty, \quad (5)$$

where M_∞ is the high-frequency (unrelaxed) longitudinal modulus and η_∞ is the high-frequency longitudinal viscosity which accounts for relaxation processes characterized by a time so short to be out of the experimental frequency window. In the low frequency (relaxed) limit, $\Delta M(\omega \rightarrow 0) = (M_0 - M_\infty) + i\omega(\eta_0 - \eta_\infty)$, where M_0 (η_0) is the zero-frequency longitudinal modulus (viscosity). In this limit, the complex longitudinal modulus becomes $M(\omega \rightarrow 0) = M_0 + i\omega\eta_0$. This is the previously described simple hydrodynamics regime, where $\eta_0 \equiv \eta_L$. In the opposite limit, the unrelaxed one, $\Delta M(\omega \rightarrow \infty) = 0$ and the longitudinal modulus takes the simple form: $M(\omega) = M_\infty + i\omega\eta_\infty$. This coincides with the Voigt model of viscoelasticity which is used since long time to describe the acoustic damping in solids (see, for instance, [44]). In this limit the spectrum takes the same form of Eq. (2), but with M replaced by M_∞ and η_L by η_∞ . The intermediate condition between the relaxed and unrelaxed limits is the one where the relaxation processes strongly couple with the acoustic waves, and the detailed description of the shape of the Brillouin spectrum requires the knowledge of the frequency dependent part of the modulus, $\Delta M(\omega)$. In this condition Eq. (2) can still be used to fit the spectrum in a narrow frequency region around the Brillouin peaks to obtain values for the "apparent" sound velocity and attenuation (see for instance, [20, 45]), i.e. their values at the frequency of the peak. This is the "traditional" way of analyzing Brillouin spectra, safe enough also for measurements obtained with low contrast and non-tandem interferometers. The analysis of the temperature behavior of these parameters gives useful information on the number and typology of relaxation processes active in the Brillouin frequency window, and will be adopted in the first part of the data analysis, paragraph IV A.

In the most general case of coupling of relaxation processes with density fluctuations, the dynamic structure factor measured with both the BLS and the IXS techniques can be expressed in terms of the generalized modulus of Eq. (5):

$$S(q, \omega) = \frac{S(q)M}{\pi\omega} \frac{M''(\omega)}{[\omega^2\rho_M/q^2 - M'(\omega)]^2 + [M''(\omega)]^2}. \quad (6)$$

In this case, the simplest possible situation is that of an exponential relaxation described by the Debye formula $\Delta M(\omega) = (M_0 - M_\infty)/(1 + i\omega\tau)$, where τ is the relaxation time. Notice that $M_0 < M_\infty$, i.e. the modulus increases with increasing frequency. The imaginary part of the modulus shows a peak at $\omega = \tau^{-1}$ corresponding to a maximum of acoustic energy absorption. It occurs,

for instance, when the frequency of the acoustic mode matches the rate of energy exchange with some internal degree of freedom. The spectral width of the peak of $M''(\omega)$ for a Debye relaxation is of 1.14 decades, in the same frequency region where the corresponding real part changes from M_0 to M_∞ (dispersion). Viscoelastic systems approaching the glass transition are characterized by a dispersion which extends in a much wider frequency range (2 or 3 decades is not a rare case). This stretching phenomenon is frequently accompanied by a power law dependence of $M''(\omega)$ which can be described by the Cole-Davidson relaxation function

$$\Delta M(\omega) = (M_0 - M_\infty)/(1 + i\omega\tau)^\beta, \quad (7)$$

where β is the stretching parameter, being $M''(\omega) \propto \omega^{-\beta}$ on the high frequency side of the peak in $M''(\omega)$. Fitting Brillouin spectra with this phenomenological ansatz for the longitudinal modulus gives the values of the amplitude ($M_0 - M_\infty$), relaxation time and stretching parameter at each measured temperature. The study of the temperature behavior of the α -relaxation parameters is the main topic of the physics of the glass transition. This is the content of Sec. V.

No mention has been given up to now of the microscopic origin of the α -relaxation. MCT suggests that in the liquid above T_g , the non-linear coupling of density fluctuations characterized by different values of q is the mechanism responsible for it. This theory gives a closed set of equations relating the dynamics of density fluctuations to the static structure factor of the same liquid. A full check of the predictions of MCT is beyond the aims of the present work. We limit ourselves to note that the Cole-Davidson relaxation function is usually adequate to represent the slow part of the relaxation function as obtained by the MCT [12] and its amplitude will be used in Section V C to check the existence of the square root singularity in the non-ergodicity factor, as predicted by the theory [12, 43].

III. EXPERIMENTAL DETAILS

A. Brillouin light scattering measurements

Glycerol of 99.5% purity purchased from Aldrich Chemicals has been employed. The sample was filtered through a $0.22 \mu\text{m}$ teflon filter directly into the cylindrical pyrex cell (inner diameter $\approx 1 \text{ cm}$) used for the measurements and slowly degassed under vacuum. The cell was sealed without breaking the vacuum. Brillouin spectra were collected in a wide temperature range comprising the whole liquid - normal and supercooled - range (melting point, $T_m = 291 \text{ K}$) down to the glassy state ($T_g = 187 \text{ K}$). The sample was placed in a copper holder which was used to regulate the temperature. For

the measurements above room temperature, the sample holder was heated with a NiCr wire using a conventional dc power supply. The temperature was controlled by a Thor Cryogenics 3010 II model temperature controller and measured by a Pt100 calibrated resistance placed close to the sample. The measurements were started after the sample temperature was thoroughly equilibrated and the temperature fluctuations were kept within $\pm 0.1 \text{ K}$ during the spectra recording. For the low-temperature measurements a Cryomech ST405 cryostat was used. The sample temperature, varied with a typical 0.5 degree/min rate, was measured with a 410-NN-1 Silicon Diode Temperature Sensor. A Coherent-Innova 300 model Ar^+ laser was operated with a typical power of $\approx 300 \text{ mW}$ on a single mode of the $\lambda_o = 514.5 \text{ nm}$ line. The light scattered by the sample was analyzed using a Sandercock-type (3+3)-pass tandem Fabry-Perot interferometer characterized by a finesse of about 100 and a contrast $> 5 \cdot 10^{10}$ [46, 47]. The elastic scattering from a dilute water suspension of Latex particles (120 nm diameter) was used to determine the instrumental resolution function $R(\omega)$. In the first part of our work, we aimed at the determination of the sound speed and attenuation of longitudinal acoustic modes. For this purpose the peak position and the linewidth (FWHM) of the Brillouin components are the only relevant parameters, making it possible to focus on the frequency region of the Brillouin peaks, where the polarized (I_{VV}) spectra replace in good approximation the isotropic (I_{ISO}) ones. In this spirit, polarized Brillouin spectra were collected in the back-scattering ($\theta \approx 180^\circ$) geometry in a wide temperature range, namely 47-441 K, using a narrow T -grid (about 5 K above room temperature, 10 K below room temperature). Different Free Spectral Range (FSR) values were used for the measurements above and below room temperature (20 GHz and $10 \div 8.3 \text{ GHz}$, respectively). The integration time was of $\approx 10 \text{ s / channel}$ and the effect of the dark counts ($< 1 \text{ count / s}$) was checked to be negligible. Typical polarized spectra covered the $0.8 \div 25 \text{ GHz}$ frequency range. In a successive step we selected some temperatures above T_g for a detailed analysis of the shape of the relaxation function. We collected in the 210-400 K temperature range (namely, 400, 350, 333, 326, 295, 285, 270, 255, 240, 225, and 210 K) polarized (I_{VV}) and depolarized (I_{VH}) spectra using two different FSRs of 13.6 GHz and 50.0 GHz in order to cover the 0.8-100 GHz frequency range. Each spectrum (polarized and depolarized) results from the overlap of the two spectra measured with different FSRs. The isotropic spectra I_{ISO} have been then obtained by subtraction of the I_{VV} and I_{VH} spectra following the procedure described in Ref. [45]. Typical I_{ISO} spectra are presented in Fig. 1 at some selected temperatures.

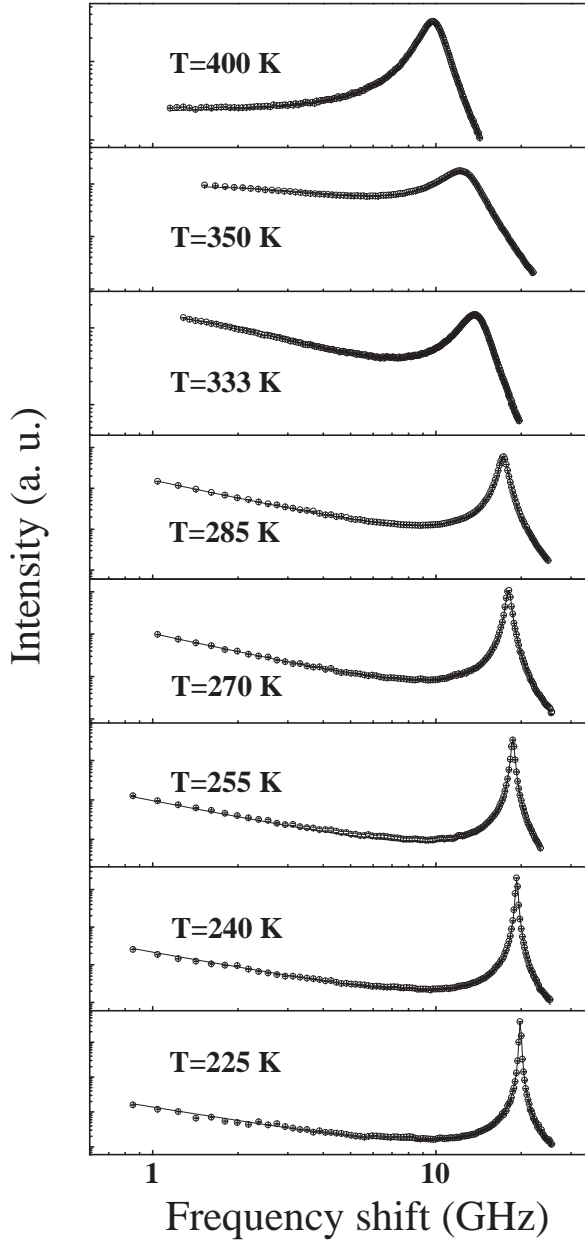


FIG. 1: Isotropic Brillouin light scattering spectra as a function of temperature for normal and supercooled liquid glycerol. The lines through the experimental points are the best fits obtained using Eqs. 6 and 14.

B. Brillouin inelastic X-ray scattering measurements

Inelastic X-ray measurements were carried out at the very high energy resolution IXS beamline (ID16) of the European Synchrotron Radiation Facility [48] using the Si(11 11 11) reflection for both the monochromator and the

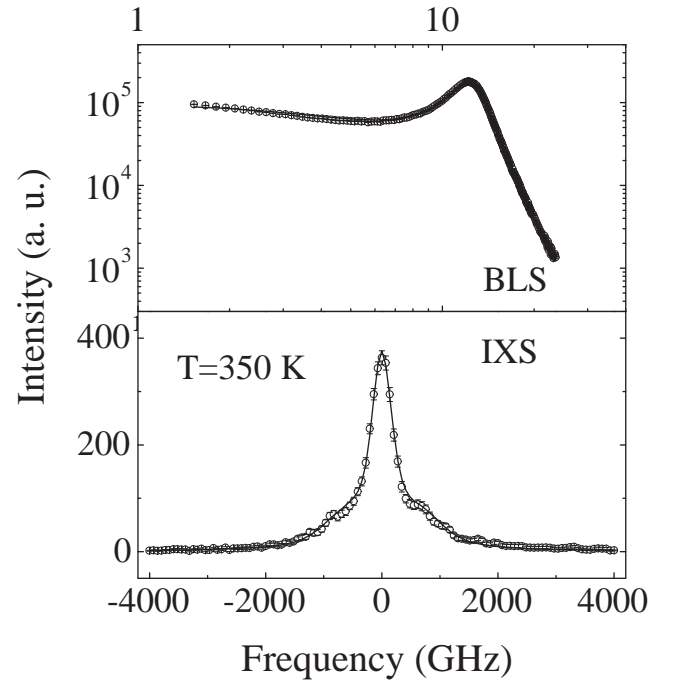


FIG. 2: A typical IXS spectrum (bottom panel) acquired at $T=350$ K and $q=2$ nm $^{-1}$ shown together with the BLS spectrum at the same temperature (top panel). The lines through the experimental points are the best fits obtained from the combined BLS-IXS analysis using Eqs. 6 and 14.

analyzers. The total energy resolution is of ≈ 1.5 meV. The IXS spectra are directly proportional to $S(q, \omega)$. IXS measurements have been performed in the 295-400 K temperature range, for q values in 2-11 nm $^{-1}$ interval, with a q -resolution of about 0.4 nm $^{-1}$. Experimental data were normalized to the intensity of the incident beam and the contribution of the empty cell was subtracted from each spectrum. A typical IXS spectrum acquired at $T=350$ K and $q=2$ nm $^{-1}$ is shown in Fig. 2 together with the BLS spectrum at the same temperature.

C. Ultrasonic measurements

The temperature behavior of the relaxed sound velocity c_0 was measured by an ultrasonic technique at 5 MHz [49], i.e. at a frequency four orders of magnitude lower than that corresponding to the LA modes revealed by Brillouin light scattering. A PZT transducer was placed deep into the sample, at a distance $L = 5$ mm from the bottom of a brass cell parallel to the surface of the transducer. The system as a whole works as an acoustic Fabry-

Perot, so that the reflection coefficient, R , shows a series of minima corresponding to the condition $L = m\Lambda/2$, where Λ is the acoustic wavelength and m is an integer number. The reflection coefficient is measured as a function of frequency by means of an HP8753A Network Analyzer. The distance $\Delta\nu$ between two neighboring minima, the free spectral range, is thus given by the relation $\Delta\nu = c/2L$, and the Fourier transform of R shows a well defined maximum at $t = 2L/c$, where c is the velocity of the acoustic wave in the sample. From the measurements of t , the velocity c of longitudinal acoustic waves was obtained at several temperatures in the range 306.5-389.5 K.

IV. DATA ANALYSIS

A. Acoustic properties of glycerol

The first step of our investigation is a traditional acoustic analysis of the Brillouin spectra consisting in the measurement of the frequency position and linewidth of the Brillouin peaks as a function of temperature. It has been shown in Sec. II A that the isotropic Brillouin spectrum, for frequencies close to those corresponding to the longitudinal acoustic (LA) peaks, can be represented by a damped harmonic oscillator (DHO) model:

$$I_{LA}(\omega) = I_{LA}^0 \frac{\Gamma_{LA}\omega_{LA}^2}{[\omega_{LA}^2 - \omega^2]^2 + [\omega\Gamma_{LA}]^2}, \quad (8)$$

where $\omega_{LA}/2\pi$ and $\Gamma_{LA}/2\pi$ correspond to the frequency position and to the full width at half-maximum (FWHM) of the LA peaks.

The spectra collected in the 47-441 K temperature range were fitted using Eq. (8) convoluted with the experimental resolution function. The values of $\omega_{LA}/2\pi$ and $\Gamma_{LA}/2\pi$ obtained with this procedure are reported in Table I. The values of the (apparent) longitudinal sound velocity and of the (apparent) longitudinal kinematic viscosity have been derived using the relations: $c = \omega_{LA}/q$ and $D = \Gamma_{LA}/q^2$, and are shown respectively in Fig. 3 and Fig. 4, where they are compared with literature data obtained from different techniques. Numerical values for c and D are reported as well in Table I. The momentum transfer q at different temperatures has been calculated (see Tab. I) using the refractive index n and the relation $q = 2nk_i$ valid in the backscattering configuration. The T -dependence of n has been evaluated from that of the mass density ρ using the Clausius-Mossotti relation. Finally, the ρ values, in the temperature range here investigated, have been obtained from the relationships:

$$\rho(T > T_g) = 1.272 - 6.55 \cdot 10^{-4}(T - 273.15), \quad (9)$$

$$\rho(T < T_g) = 1.332 - 3.20 \cdot 10^{-4}(T - 187), \quad (10)$$

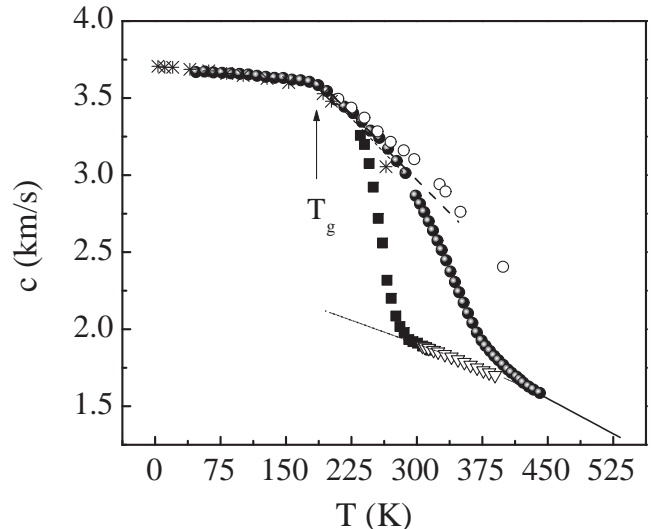


FIG. 3: Sound velocity data from the present Brillouin light scattering experiment (full circles) compared with literature data: stars represent previous BLS measurements from [32], full squares represent ultrasonic measurements at 15 MHz from [23]. Limiting high frequency values obtained from our BLS full spectrum analysis are reported as open circles, together with the expressions given in Refs. [23, 24, 28, 30] (dash-dot line). Limiting low frequency data determined from our US measurements are reported as open triangles together with linear expressions given in Refs. [23, 24, 28, 30] (full line).

with T in K and ρ in g/cm^3 . Eq. (9) is from Ref. [24], and Eq. (10) has been obtained using the thermal expansion coefficient of the glass at 180 K, $\alpha_{\text{glass}} = 2.4 \cdot 10^{-4} \text{ K}^{-1}$ [14].

Looking at figures 3 and 4, it can be seen that our data show the well-known features expected in presence of the structural relaxation process: a marked dispersion of the sound velocity, accompanied by a maximum of the absorption. In particular, the hypersonic velocity shows the typical S -shape dispersion curve (full circles) that is bounded by the limiting high (unrelaxed) and low (relaxed) frequency values of the velocity, c_∞ and c_0 , respectively. The change in the slope of $c(T)$ at about 187 K indicates the occurrence of the liquid-glass transition. We report in the same figure the values obtained by ultrasonic measurements of the longitudinal modulus (squares) [23] showing that a change of the probing frequency from the MHz to the GHz domain moves the dispersion region towards higher temperatures and broadens the temperature region where the α relaxation is active. Fig. 3 also shows different linear extrapolations of the unrelaxed adiabatic velocity taken from Refs. [24, 28, 30] (dash-dot line), together with the values of c_∞ obtained from the full spectrum analysis (open

TABLE I: Peak position ($\omega_{LA}/2\pi$) and FWHM ($\Gamma_{LA}/2\pi$) of the Brillouin peak reported in the whole range of the investigated temperatures. These parameters have been determined by fitting the spectral region around the Brillouin peak using the DHO model, Eq. (8), convoluted with the instrumental resolution. The values of FWHM for temperatures lower than 196 K have not been reported because, on decreasing the temperature, the linewidths become too small, with respect to the resolution function, to be reliably extracted. Column 2 reports the values of the exchanged momentum q . Columns 4 and 6 report the longitudinal sound velocity and the longitudinal kinematic viscosity, respectively.

T [K]	q [nm ⁻¹]	$\omega_{LA}/2\pi$ [GHz]	c [m/s]	$\Gamma_{LA}/2\pi$ [GHz]	D [cm ² /s]
47.0	0.0373	21.80	3668	—	—
57.0	0.0373	21.80	3672	—	—
67.0	0.0373	21.74	3666	—	—
77.0	0.0372	21.70	3663	—	—
87.0	0.0372	21.66	3659	—	—
97.0	0.0372	21.62	3656	—	—
107.0	0.0371	21.58	3652	—	—
117.0	0.0371	21.51	3643	—	—
127.0	0.0371	21.45	3637	—	—
137.0	0.0370	21.39	3631	—	—
147.0	0.0370	21.36	3630	—	—
157.0	0.0369	21.28	3619	—	—
166.0	0.0369	21.23	3614	—	—
177.0	0.0369	21.16	3605	—	—
187.0	0.0368	21.01	3583	—	—
197.0	0.0367	20.73	3546	0.09	0.004
207.0	0.0366	20.36	3490	0.10	0.005
217.0	0.0366	20.06	3444	0.13	0.006
227.0	0.0365	19.77	3402	0.18	0.009
237.0	0.0364	19.41	3347	0.25	0.012
247.0	0.0364	19.04	3288	0.32	0.015
257.0	0.0363	18.72	3241	0.45	0.022
267.0	0.0362	18.28	3171	0.66	0.031
277.0	0.0362	17.79	3092	0.90	0.043
287.0	0.0361	17.31	3013	1.19	0.058
298.6	0.0360	16.43	2866	1.88	0.091
303.7	0.0360	16.11	2813	2.13	0.104
308.6	0.0359	15.78	2760	2.38	0.116
313.7	0.0359	15.42	2700	2.65	0.129
318.6	0.0359	15.07	2640	2.87	0.140
323.7	0.0358	14.68	2575	3.18	0.156
328.6	0.0358	14.32	2514	3.43	0.168
333.6	0.0358	13.93	2447	3.60	0.177
338.6	0.0358	13.50	2374	3.87	0.190
343.6	0.0357	13.10	2306	3.96	0.196
348.6	0.0357	12.71	2239	4.12	0.203
353.7	0.0357	12.31	2172	4.13	0.204
358.6	0.0356	11.91	2103	3.99	0.198
363.7	0.0356	11.54	2040	3.87	0.192
368.8	0.0355	11.18	1978	3.68	0.183
374.3	0.0355	10.88	1927	3.39	0.169
378.8	0.0355	10.67	1892	3.21	0.148
383.8	0.0354	10.48	1858	2.96	0.139
388.8	0.0354	10.28	1826	2.77	0.130
393.7	0.0353	10.12	1799	2.59	0.120
399.0	0.0353	9.94	1769	2.37	0.110
404.3	0.0353	9.75	1738	2.17	0.104
408.5	0.0352	9.63	1717	2.06	0.096
414.4	0.0352	9.48	1691	1.90	0.090
418.4	0.0352	9.36	1672	1.77	0.084
422.1	0.0352	9.24	1652	1.64	0.077
428.2	0.0351	9.09	1628	1.51	0.072
433.8	0.0351	8.97	1608	1.41	0.066
441.0	0.0350	8.84	1586	1.30	0.061

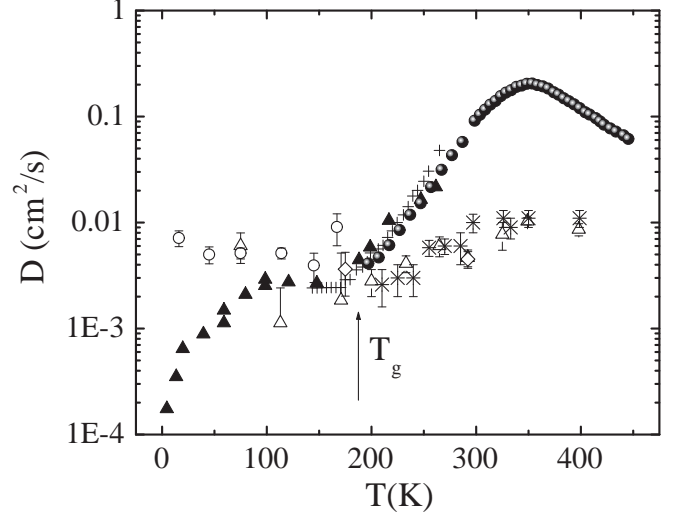


FIG. 4: Apparent kinematic viscosity Γ_{LA}/q^2 derived from the analysis of the Brillouin spectrum (full circles) compared with literature data. Crosses are from Ref. [30], full triangles from Ref. [32]. Limiting high frequency values from Refs. [39, 40, 41] are reported as diamonds, open triangles, and open circles respectively. Stars are the unrelaxed values determined from the BLS full spectrum analysis presented here.

circles) which will be presented in the next section. Finally, Fig. 3 reports values of the relaxed sound velocity, whose temperature behavior is essential for the full spectrum analysis of Sec. IV B. In particular, several sets of data for c_0 are available in the literature [24, 28, 30], obtained in different and narrow temperature ranges below 360 K and above 440 K. They are typically described by almost linear trends with different slopes. In addition, we present here new ultrasonic data measured in an intermediate temperature range between 306.5 K and 389.5 K. These data are magnified in Fig. 5 and the parameters for the linear approximation of c_0 in different temperature regions are reported in Tab. II. Once these partial sets of data are shown all together in Fig. 5, a globally non-linear behavior of $c_0(T)$ becomes clear, similar to that observed in many glass-formers [50]. Conversely, when we plot $M_0 = \rho c_0^2$, as a function of T (inset of Fig. 5), this quantity can be reasonably fitted by a straight line in a wide T -range from 245 to 505 K. The parameters of the fit are reported in Tab. II. This linear behavior of $M_0(T)$ is in agreement with what observed by Christensen and Olsen in a restricted temperature region [51].

Focusing now our attention on the longitudinal kinematic viscosity, the well defined maximum close to 350 K in Fig. 4 corresponds to the matching between the relaxation rate and the characteristic frequency of the longitudinal acoustic excitations. In the same figure we report as well the values of D determined by different

TABLE II: Temperature dependence of c_0 and M_0 (T is in Kelvin).

Parameter	Formula	Units	T - range	Refs.
c_0	$2519 - 2.051 T$	m/s	232-343 K	[24]
c_0	$2518 - 2.045 T$	m/s	200-360 K	[28]
c_0	$2918 - 3.041 T$	m/s	440-534 K	[30]
c_0	$2593 - 2.286 T$	m/s	307-390 K	^a
M_0	$8.110 - 1.183 \times 10^{-2} T$	GPa	245-505 K	^a

^aPresent work.

techniques. Particularly relevant is the comparison with x-ray scattering data. Generally, the IXS probing frequency is so high that, especially for low temperatures, the structural relaxation is definitively out of the spectral window. Therefore, IXS typically probes the unrelaxed values of Γ/q^2 , i.e. η_∞/ρ . Fig. 4 shows that the kinematic viscosity data obtained by BLS and IXS are consistent, within their error-bars, in a range of about 80 K below T_g beside the fact that they correspond to q^2 values which differ by a factor 10^3 . Below T_g , the structural relaxation is located at frequencies lower than one Hz, and we cannot expect any significant contribution from it to the acoustic loss in the GHz region. The absence of an excess damping in BLS data over the IXS unrelaxed ones at T_g points in favor of an α relaxation-only scenario for the dynamics of glycerol. This is a peculiar behavior of glycerol, and, possibly, of associated liquids, different from that observed in several fragile systems like OTP, DGEBA and PB [52], where the presence of an excess attenuation in the GHz range reflects the coupling of the LA modes with internal, molecular degrees of freedom, giving rise to fast relaxation processes of thermal nature. Below 100 K, the BLS values of D [32] start to decrease, suggesting a scaling of Γ with a power of q higher than 2. A dynamic contribution to the sound attenuation having influence on low frequency density fluctuations has been recently proposed as the origin of this phenomenon [41, 53].

Additional information on the number and nature of the relaxation processes active in glycerol can be obtained from the high temperature-low frequency non dispersive region. This regime is well described by simple hydrodynamics [14], and the acoustic absorption, in low thermally conducting liquids, is given by:

$$\alpha = \omega^2 \frac{\eta_L}{2\rho c^3} \quad (11)$$

where $\eta_L = \eta_b + 4/3\eta_s$ and η_L , η_b , and η_s are the longitudinal, bulk and shear viscosity, respectively. In simple liquids, where η_b is small, η_s gives the most important contribution to the acoustic attenuation, giving rise to the so-called classical absorption [14]:

$$\alpha_{cl} = \frac{2}{3}\omega^2 \frac{\eta_s}{\rho c^3} \quad (12)$$

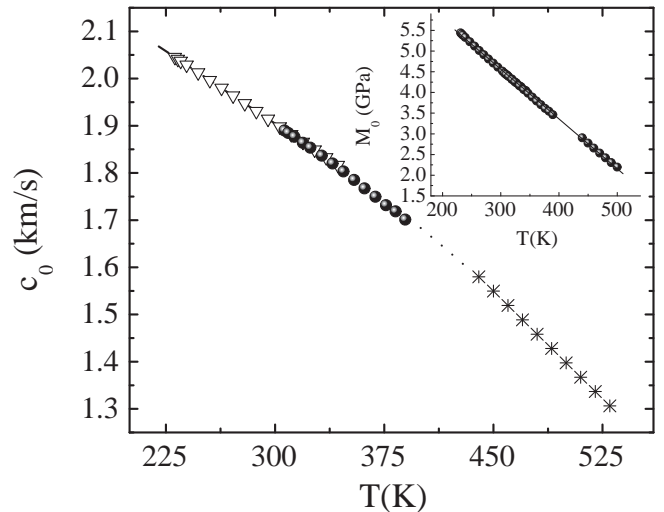


FIG. 5: Relaxed sound velocity. Our c_0 measurements collected at 5 MHz are reported as full circles and are compared with previous determinations: triangles refer to measurements reported in Ref. [24, 28] and stars represent the linear expression given in Ref. [30]. This whole set of data does not show a linear behavior. However the same data, once reported in terms of relaxed longitudinal modulus, M_0 , do show a linear behavior, as reported in the inset of the figure. The linear representation of M_0 is reported in terms of c_0 as dotted line.

From Eq. (11) and Eq. (12), the relationship between the longitudinal and the shear viscosity can be easily written as:

$$\frac{\eta_L}{\eta_s} = \frac{4}{3} \frac{\alpha}{\alpha_{cl}} \quad (13)$$

A different temperature behavior of the α/α_{cl} ratio distinguishes Kneser and associated liquids [14]. The Kneser-type systems, as for example ionic liquids and the majority of organic liquids, show a temperature dependent α/α_{cl} ratio ranging between 3 and 400. In these liquids, the excess absorption over the classical value is due to exchange of energy between internal (rotations and vibrations) and external (acoustic modes) degrees of freedom, showing a marked temperature dependence [14]. On the contrary, for the associated liquids, often characterized by CH_3 , CH_2 , and OH groups, the bulk viscosity is essentially only related to the structural relaxation, the contributions coming from the internal degrees of freedom being negligible. In these systems, the acoustic measurements performed in the non-dispersive region show a temperature independent ratio α/α_{cl} lying between one and three [14]. In particular, for glycerol, it has been proven that the α/α_{cl} ratio is approximately constant and equal to 1.78 [14].

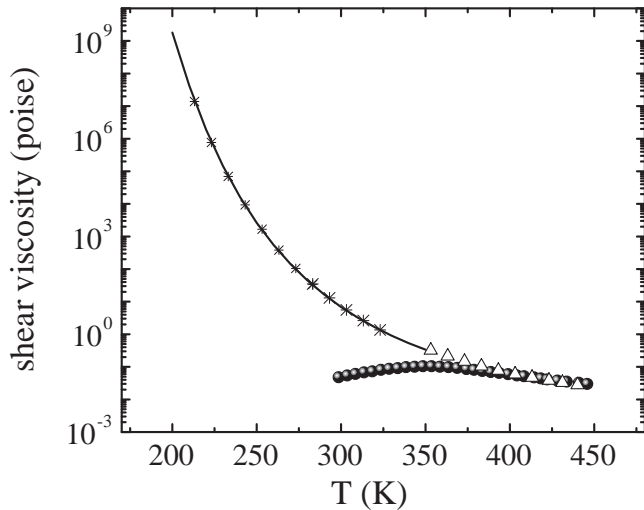


FIG. 6: Shear viscosity determined from our Brillouin data as $\eta_S = \eta_L/2.4 = \Gamma_{LA}\rho/2.4q^2$ (full circles). These values are compared with those obtained from direct shear viscosity measurements: triangles refer to measurements reported in Ref. [54], stars represent measurements from Ref. [55], and the straight line indicates the expression reported in Ref. [24].

On this basis, starting from the values of η_L obtained from the present BLS data, and assuming the same temperature dependence for shear and volume viscosity, η_S has been obtained using the Eq. (13), and $\alpha/\alpha_{cl} = 1.78$ [14]. In Fig. 6 we report such an evaluation for η_S together with viscosimetric measurements [24, 54, 55]. In the high temperature region, the two data sets show a common trend, reinforcing the hypothesis that no fast thermal relaxations are responsible of the dynamics of glycerol, at least in the frequency and temperature regions covered by Brillouin light scattering. This statement is even more clear if Fig. 6 is compared with Fig. 7 of Ref. [20], where $D(T)$ for the Kneser liquid OTP is reported. In this latter case, a marked temperature dependent α/α_{cl} ratio has been observed, attributed to the effects of a thermal relaxation, whose presence has been recently supported by molecular dynamics simulations [22].

B. Full spectrum analysis

The traditional analysis, presented in previous section, helps us to choose an ansatz for the frequency dependent longitudinal acoustic modulus $M^*(\omega)$. To this respect, the most relevant indications we gained from this approach are: *i*) at temperatures close to the glass transition the (apparent) kinematic viscosity obtained from BLS is consistent with the corresponding unrelaxed val-

ues determined by IXS, and *ii*) in the high temperature limit the shear viscosity estimated from BLS collapses on that obtained by viscosimetric measurements. Both these results indicate the absence of thermal relaxations in glycerol, in agreement with what inferred some 40 years ago on the basis of ultrasonic measurements [14]. Therefore, in order to model $M^*(\omega)$, we may suppose that the structural relaxation is enough to catch the leading contributions to the relaxational dynamics of glycerol in the GHz frequency window. Relaxation processes so fast to be out of the experimental frequency window are described by an instantaneous term in the modulus function and their effects are taken into account by the unrelaxed viscosity η_∞ . Following these indications, our ansatz for the $M^*(\omega)$ function consists of a Cole-Davidson function for the α relaxation plus an instantaneous contribution:

$$M^*(\omega) = M_\infty + \frac{(M_0 - M_\infty)}{(1 + i\omega\tau_\alpha)^\beta} + i\omega\eta_\infty. \quad (14)$$

Substituting this expression for $M^*(\omega)$ into Eq. 6, we have obtained a model function to fit to the BLS spectra. In particular, this full spectrum analysis has been carried out for temperatures higher than T_g , adopting the following procedure: (i) The thermal diffusion contribution is considered as a Dirac δ term centered at zero frequency, whose amplitude is proportional to that of the adiabatic part of the spectrum via the LP-ratio. In fact the characteristic time of the thermal diffusion mode as measured, for instance, in Ref. [31] and properly rescaled to the q values accessed to by BLS is located at about 10 ns, i.e. more than three decades far from the Brillouin peak in the whole temperature region considered here. Moreover, even at the highest investigated temperatures, if the thermal contribution is explicitly considered as a Lorentzian peak centered at zero frequency, the quality of the fit is unchanged together with the values of the fitting parameters. (ii) The values of the relaxed adiabatic sound velocity c_0 have been fixed to those reported in Tab. III. (iii) η_∞/ρ has been left to vary in the fit having as starting point the value determined by IXS [39, 40, 41]. The weak T-dependence and the experimental uncertainty of IXS data discouraged us from fixing η_∞/ρ to a constant value. (iv) The unrelaxed adiabatic sound velocity c_∞ has also been taken as an adjustable parameter in the whole T-range, while τ_α , and β have been considered free or fixed depending on the temperature region investigated. In particular, in the low temperature region ($T \leq 255$ K), being the structural relaxation out of the Brillouin window, τ_α was fixed and β left free since it affects the shape of the Mountain region of the spectrum. In this region τ_α has been imposed to be proportional to the shear viscosity η_S , i.e. $\tau_\alpha = J\eta_S$, where J is a constant coefficient having the dimensions of a compliance (see for example Ref. [20]). In contrast, in the highest temperature region ($T \geq 270$ K) the structural relaxation becomes progressively active in the GHz frequency window, so that we are able to obtain τ_α from the fit, but

we need to fix the value of β . Its value has been chosen within the limits suggested from Ref. [25], i.e. 0.40 ± 0.05 , and also consistent with our results at lower T . For some selected temperatures, namely 295 K, 350 K, and 400 K, we simultaneously fit BLS ($q=0.036 \text{ nm}^{-1}$) and IXS ($q=2 \text{ nm}^{-1}$) spectra, following the combined fitting procedure described in Ref. [18]. In this procedure we use a single IXS spectrum collected at $q=2 \text{ nm}^{-1}$, since the spectra at higher q 's progressively depart from the hydrodynamic regime. In the joint-analysis, the values of c_∞ and η_∞ are mainly related to the position and linewidth of the Brillouin peaks of the IXS spectra, while τ_α and β are mainly related to the shape of BLS spectra. The obtained best fitting curves are shown in Fig. 1 and Fig. 2 as full lines. The whole set of fitting parameters is reported in Tab. III. The relaxation times obtained from the BLS data-analysis are also shown in Fig. 7 together with several literature data. In particular, in the same figure we report three different evaluations of τ_α for $T=350 \text{ K}$: the value obtained from the described fit procedure (full circle); the value of τ_{max} (down triangle) corresponding to the maximum of the Cole-Davidson function used to model the BLS spectra; and the characteristic time of longitudinal acoustic mode $\tau_{LA} = 1/2\pi\nu_{LA}$ (star), i.e. the time corresponding to the maximum of the BLS absorption data in Fig. 4. We underline that this last evaluation of τ_α is model independent. Fig. 7 shows that, at $T=350 \text{ K}$, τ_{max} and τ_{LA} coincide. This result represents a strong support of the reliability of the values of the structural relaxation time as deduced from the full spectrum analysis presented here.

V. DISCUSSION

A. The structural relaxation time and the stretching parameter

The temperature behavior of the structural relaxation time determined in the previous paragraph is compared with that obtained by different spectroscopic techniques (dielectric spectroscopy, impulsive stimulated Brillouin scattering, impulsive stimulated thermal scattering, ultrasonic techniques, depolarized light scattering) in Fig. 7. The inset of the figure shows that the data obtained by these techniques, once rescaled by a constant, collapse into a single master curve, indicating that the α -scale universality is obeyed in glycerol in a wide time-temperature range. A simple explanation for the difference in the absolute values of τ is the different microscopic correlators measured by the different techniques. Next in importance is the definition of the characteristic time itself. In some cases, like in BLS and ultrasonic measurements, the longitudinal acoustic modulus formalism has been used, with a specific CD complex function to describe the structural relaxation process. In some other case, like in dielectric spectroscopy measurements, the compliance formalism was chosen and, al-

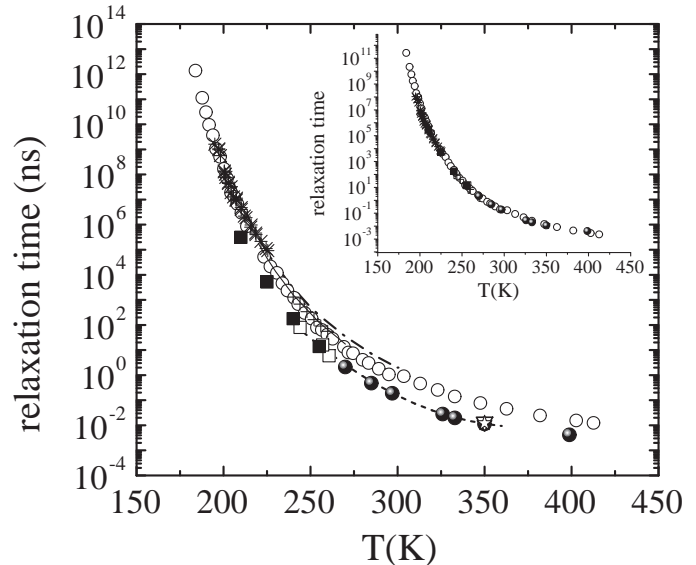


FIG. 7: Structural relaxation time of glycerol from the BLS full spectrum analysis compared with various literature data. Full circles and squares represent our BLS values obtained in the fitting procedure by leaving the τ_α parameter free or by imposing it to be proportional to the shear viscosity, respectively. The star represents the value τ_{LA} corresponding to the maximum of the acoustic attenuation for the longitudinal modes; the down triangle marks the value of τ_α at 350 K corresponding to the maximum of the Cole-Davidson function used to model the BLS spectra. The open squares represent ultrasonic data taken at 2, 10, and 27 MHz [25], pluses are from Ref. [31], crosses are from Ref. [56], open circles are from Ref. [37]. The short-dashed line is the polynomial law given in Ref. [28]. The dash-dot line is the Vogel-Fulcher equation reported in Ref. [26] describing photon correlation data. The solid line is the Vogel-Fulcher equation obtained in Ref. [29] from a fit to ISTS data. In the inset, the same data are reported after rescaling by a constant. The collapse of all the data on a single master-curve indicates the validity of the α -scale universality in glycerol over a wide time-temperature region.

though a CD relaxation function was used, its parameters are not analytically related to those of the CD modulus function. Moreover, some authors reports the values of τ_α directly obtained from the fit [26, 28, 56]; others report the average value $\langle \tau \rangle$ ($\beta\tau$, in case of a CD function; $(\tau/\beta)\Gamma(1/\beta)$, where Γ is the Gamma function, in the case of a Kolhraush-Williams-Watt function) [29, 31]; others report the value corresponding to the maximum of the absorption τ_{max} [25, 37].

Despite these technical obstacles, one reasonably expects that, at least in those cases where the same correlator is measured, a quantitative agreement between relaxation times obtained by different techniques should be reached. In particular BLS, ultrasound, ISBS, and ISTS all probe density fluctuations. The agreement between BLS, ultrasonic, and ISBS τ -modulus data (present work,

TABLE III: Parameters of the full spectrum analysis of liquid and supercooled glycerol at the temperatures reported in column 1. Columns 2, 3, and 4 report respectively the characteristic time of the α -CD function, the stretching parameter, and the average value of τ determined as $\langle\tau_\alpha\rangle = \beta\tau_\alpha$. Columns 5 and 6 report the high and low limiting values of the sound velocity, respectively. Column 7 reports the instantaneous kinematic viscosity contribution.

T [K]	τ_α [10^{-12} s]	β	$\langle\tau_\alpha\rangle$ [10^{-13} s]	c_∞ [m/s]	c_0 [m/s]	η_∞/ρ [10^{-3} cm/s ²]
210	1.3×10^9 ^a	0.24	3.1×10^9	3495	2088 ^c	2.7
225	1.9×10^7 ^a	0.27	5.1×10^7	3437	2056 ^c	3.3
240	6.3×10^5 ^a	0.28	1.8×10^6	3372	2027 ^c	2.7
255	4.0×10^4 ^a	0.34	1.4×10^5	3283	1996 ^c	5.8
275	6.0×10^3 ^b	0.35	2.1×10^4	3222	1965 ^c	5.8
285	1.3×10^3 ^b	0.37	4.8×10^3	3160	1933 ^c	6.1
295	5.1×10^2 ^b	0.37	1.9×10^3	3105	1919 ^d	9.0
326	7.7×10^1 ^b	0.36	2.8×10^2	2941	1848 ^d	11.0
333	5.4×10^1 ^b	0.36	2.0×10^2	2894	1832 ^d	9.0
350	3.1×10^1 ^b	0.36	1.1×10^2	2762	1793 ^d	11.0
400	1.2×10^1 ^b	0.36	4.1×10^1	2404	1675 ^e	11.0

^aFixed on the basis of the temperature behavior of the shear viscosity.

^bFree parameter in the fit.

^cRef. [24].

^dPresent work.

^eValue obtained from the interpolation of our data of c_0 and those reported in Ref. [30].

[25], [28]) is evident in Fig. 7. Different from this, ISTS τ -compliance data [29, 31] are shifted by about a factor ten towards longer times. Even after a conversion of the BLS data to the compliance formalism, a shift of about a factor three persists between the BLS and the ISTS data. At present, we cannot find any explanation for this interesting anomaly, and we limit ourselves to suggest to perform this comparison on other glass-forming systems.

The present full spectrum analysis provides information also on the T -dependence of the shape parameter β_{CD} of the α -relaxation function. In particular, an almost constant value, namely 0.37 ± 0.03 , was found for temperatures between 270 and 400 K, close to the value 0.40 ± 0.05 obtained in a previous ultrasonic investigation [25]. The value of the stretching parameter decreases with temperature, as shown in Tab. III - the same trend being also found in the dielectric investigation reported in Ref. [37], the only one which covers an extremely wide temperature-frequency range. For a quantitative comparison with the values obtained by other techniques where compliance relaxation functions are used, like ISTS, photon correlation spectroscopy, and specific heat spectroscopy, we converted our modulus-based data into compliance-based data obtaining the values reported in Tab. IV. Moreover, for those techniques where the stretching parameter was referred to a Kohlrausch-Williams-Watt function (KWW), we have transformed β_{KWW} into β_{CD} using the equations reported in Ref. [57]. Our BLS data compare fairly well with an average value of $\beta_{CD} = 0.45 \pm 0.05$ estimated from ISTS measurements at different T and exchanged mo-

TABLE IV: Summary of the shapes of different compliance functions.

Technique	β_{CD}	Temperature range	Refs.
BLS	0.40 ± 0.05	210 K	present work
BLS	0.40 ± 0.05	225 K	present work
BLS	0.53 ± 0.05	240 K	present work
BLS	0.56 ± 0.05	255 K	present work
ISTS	0.45 ± 0.05	200-340 K	[29, 31]
PCS	0.40 ± 0.03	195-225 K	[26, 27]
Ultrasonics	0.42 ± 0.05	235-300 K	[25]
Specific heat	0.51 ± 0.03	195-225 K	[58]
Dielectrics	$0.55 \div 0.65$	195-300 K	[37]

mentum, $\beta_{CD} = 0.40 \pm 0.05$ from PCS data [26, 27] and $\beta_{CD} = 0.51 \pm 0.03$ from specific heat spectroscopy data [58].

B. The limiting high frequency sound velocity

The limiting high frequency values of the adiabatic sound velocity obtained from the fit of the Brillouin spectra are shown in Fig. 8. In the same figure, we report two different ansatzs for the unrelaxed speed of sound obtained assuming either a linear T -dependence of M_∞ [24] or a linear T -dependence of c_∞ [28, 30]. In Ref. [30], using stimulated Brillouin gain spectroscopy, a slight but continuous curvature in the c_∞ data was observed and two different expressions were reported. Our values of

c_∞ agree with those given in Ref. [30] for the 185.5-281.4 K temperature range (stars in Fig. 8). However, we observe that an extrapolation of this equation to higher temperatures is not able to reproduce our BLS results. In the cases of Refs. [24, 28], the linear expressions reported in Fig. 8 are derived as extrapolations of the data collected at low frequencies, in a region where, possibly, complete unrelaxed conditions are not fulfilled. The values of c_∞ obtained from the present BLS analysis display a slope smaller than in previous determinations and a decreasing trend on increasing temperature with a possible change of regime at about 310 K. This estimation is in remarkable agreement with a previous IXS determination, namely $T_x = 300 \pm 20$ K [40], which was suggested to mark the microscopic transition between two different dynamical regimes related to the glass and liquid phases, respectively.

It is interesting to notice that a different representation can be given for the same data by plotting the longitudinal modulus $M_\infty = \rho c_\infty^2$ as a function of T . The inset of Fig. 8 shows that $M_\infty(T)$ can be reasonably approximated by the linear behavior $M_\infty(T) = [26.2(2) - 0.05(1)T]$ GPa. This is similar to what found for the T -dependence of the limiting shear modulus of glycerol [59]. This linear behavior of the unrelaxed moduli is not universal in supercooled liquids. Indeed, in many glass-formers, a linear extrapolation leads to unphysical low values of M_∞ in the relaxation region. Rather, the limiting compliance J_∞ , the reciprocal of M_∞ , is found often to vary linearly with temperature [2, 50].

C. The non-ergodicity factor

A detailed analysis in terms of the predictions of the mode-coupling theory is beyond the subject of this work, we only present here an estimation of the non ergodicity parameter, f , derived from our isotropic Brillouin spectra. With BLS, in fact, we directly probe the density-density correlators, and thus we can extend the temperature interval recently investigated in Ref. [29]. In the zero exchanged momentum limit, $q \rightarrow 0$, the non-ergodicity factor, f_q , can be calculated via the equation $f_0 = 1 - c_0^2/c_\infty^2$ [43]. This is equivalent to integrate the Mountain peak in quasi elastic light scattering spectra or the quasi elastic peak in neutron scattering spectra. Therefore, the f_0 parameter has been calculated from the c_0 and c_∞ values reported in Tab. III. The temperature interval investigated here, namely 210-400 K, includes several previously different T_c estimations. Looking at Fig. 9, it is evident that f_0 decreases with increasing temperature, but no signature of a cusp-like behavior emerges in glycerol. Fig. 9 also shows that our results are consistent with those recently obtained by Paolucci and Nelson [29] who measured the non-ergodicity factor from the strength of the structural relaxation using the ISTS technique in the 228-268 K temperature range. However, although the existence of the critical temperature cannot

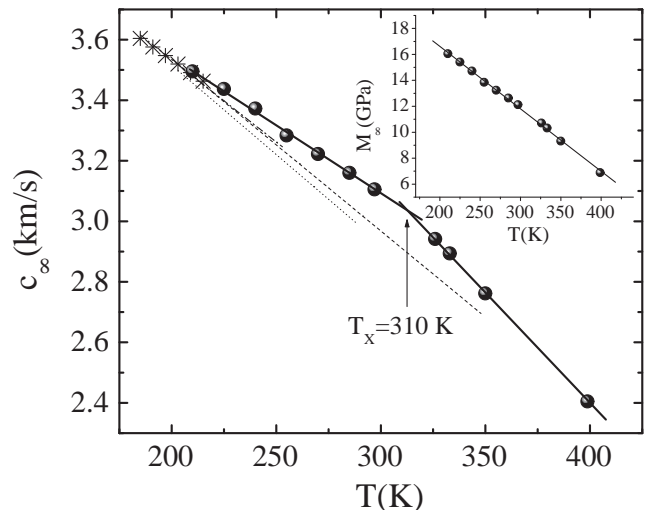


FIG. 8: Unrelaxed sound velocity. The values of c_∞ determined from the BLS full spectrum analysis (full circles) are compared with various proposed extrapolations: dashed, dotted, and dash-dot lines are from Refs. [28], [24], and [30], respectively. Stars represent data of c_∞ from the linear expression given in Ref. [30] in the 185.5-218.4 K temperature range. Solid lines are a guide for the eye. In the inset circles represent the unrelaxed longitudinal modulus $M_\infty = \rho c_\infty^2$. The solid line represents the equation obtained by a linear fit of the modulus data: $M_\infty(T) = [26.2 \pm 0.2 - 0.05 \pm 0.01 T]$ GPa.

be supported here, we consider this check only a preliminary test of the MCT predictions, and it is not possible to exclude the validity of a "non-idealized" mode-coupling description for glycerol.

VI. CONCLUSIONS

Brillouin light scattering measurements of glycerol have been presented, performed in a wide temperature region ranging from the high temperature liquid to the glassy state. Our investigation was aimed at understanding the dynamics of density fluctuations in a prototypical intermediate glass-former in the high frequency region where the precursor of the glass transition, i.e. the structural relaxation, is present above T_g . The associated nature of glycerol plays in favor of a simple relaxation pattern, where the additional effects of internal thermal relaxations is negligible in the GHz region. Focusing on the narrow frequency region of the Brillouin peak, the temperature behavior of the characteristic frequency and lifetime of the longitudinal acoustic modes has been analyzed. In particular, we have drawn the attention on the behavior of the apparent kinematic viscosity that, at

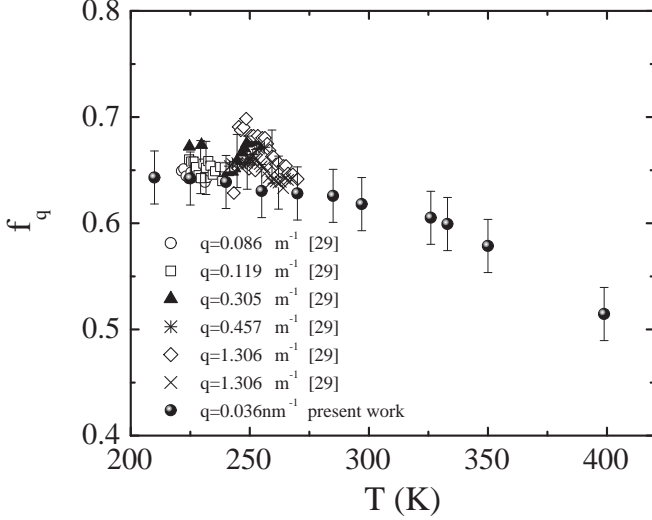


FIG. 9: The non-ergodicity factor in glycerol as a function of temperature. The values of f_0 determined from our BLS full spectrum analysis are compared with the data collected at different wavevectors and reported in Ref. [29].

temperatures close to and below T_g , approaches the unrelaxed value estimated from IXS data. Different from glass forming systems that show secondary relaxations of intramolecular nature, no excess of attenuation for the longitudinal acoustic modes has been revealed near the glass transition temperature. Moreover, the longitudinal to shear viscosity ratio is found to be almost temperature independent in the non-dispersive high-temperature region. These findings suggest that an α -relaxation only model plus an instantaneous viscosity term are able to

catch the leading contributions to the dynamics of the density fluctuations. The choice of this model was also supported by a combined analysis of light and inelastic x-ray scattering spectra. Starting from this guess, we analyzed high-resolution BLS spectra over two decades in frequency (full spectrum analysis) and we were able to obtain details on the relaxation parameters from the shape of the Brillouin peaks and of the Mountain region of the spectrum.

The temperature behavior of the structural relaxation time, $\tau_\alpha(T)$, obtained by this fitting procedure, has been compared with the results coming from different spectroscopic techniques. The α -scale universality is obeyed for the structural process, i.e. the values of τ_α are proportional to those revealed by different experimental techniques. Moreover, a significant difference of the absolute values of our τ_α data is observed with respect to those obtained by ISTS, a technique which probes the density fluctuations as well. At the moment, we have no explanation for this anomaly. It would be interesting to investigate whether this anomaly holds for other glass-formers as well. Finally, preliminary considerations have been presented on the predictions of the mode coupling theory. In particular, in the analysis presented here, the calculated non-ergodicity factor, f_0 , is found to decrease with increasing temperature, but no signature of a cusp-like behavior is revealed in glycerol. We can thus argue that the predictions of the idealized MCT are not fulfilled in this system. Of course, this does not imply that MCT is not appropriate to describe the dynamics of glycerol. Instead, this suggests that a more complete version of the theory should be applied in this case. To this respect, the model introduced by Franosch et al. [60], including both linear and quadratic coupling contributions and tested on depolarized light scattering spectra of glycerol, seems to be a suitable candidate to be tested on spectra of density fluctuations. Work along this line is in progress.

-
- [1] For glass forming polymers see, for instance, C.H. Wang, G. Fytas and J. Zhang, *J. Chem. Phys.* **82**, 3405 (1985), and references therein; L. Börjesson, J.R. Stevens and L.M. Torell, *Polymer* **28**, 1803 (1987).
 - [2] For molten salts and mixtures see, for instance, L.M. Torell, D.C. Ziegler and C.A. Angell, *J. Chem. Phys.* **81**, 5053 (1984); L.M. Torell, *J. Chem. Phys.* **76**, 3467 (1982).
 - [3] For simple viscoelastic liquids see, for instance, P.J. Carroll, and G.D. Patterson, *J. Chem. Phys.* **81**, 1666 (1984).
 - [4] G. Floudas, G. Fytas and I. Alig, *Polymer* **13**, 2307 (1991).
 - [5] R.D. Mountain, *Rev. Mod. Phys.* **38**, 205 (1966); R.D. Mountain, *J. Res. Natl. Bur. Std.* **70A**, 207 (1966).
 - [6] C.J. Montrose, V.A. Solov'yev, and T.A. Litovitz, *J. Acous. Soc. Amer.* **43**, 117 (1967).
 - [7] J.P. Boon, and S. Yip, *Molecular Hydrodynamics*, Dover Publications Inc., New York (1991).
 - [8] C. Dreyfus, M.J. Lebon, H.Z. Cummins, J. Toulouse, B. Bonello, and R.M. Pick, *Phys. Rev. Letters* **69**, 3666 (1992).
 - [9] L.M. Torell, L. Börjesson and M. Elmroth, *J. Phys.: Condens. Matter* **2**, SA207 (1990).
 - [10] C. Dreyfus, M.J. Lebon, F. Vivicorsi, A. Aouadi, and R.M. Pick, *Phys. Rev. E* **63**, 041509 (2001).
 - [11] M. Soltwisch, J. Sukmanowski, and D. Quitmann, *J. Chem. Phys.* **86**, 3207 (1987).
 - [12] For a review, see: W. Götze and L. Sjögren, *Rep. Prog. Phys.* **55**, 241 (1992).
 - [13] N.J. Tao, G. Li, and H.Z. Cummins, *Phys. Rev. B* **43**, 5815 (1991); N.J. Tao, G. Li, and H.Z. Cummins, *Phys. Rev. B* **45**, 686 (1992); G. Li, W.M. Du, J. Hernandez, and H.Z. Cummins, *Phys. Rev. E* **48**, 1192 (1993); W.M. Du, G. Li, and H.Z. Cummins, M. Fuchs, J. Toulouse and L.A. Knauss, *Phys. Rev. E* **49**, 2192 (1994); A. Brodin, M. Frank, S. Wiebel, G. Shen, J. Wuttke,

- and H.Z.Cummins, Phys. Rev. E **65**, 051503 (2002).
- [14] K.F. Herzfeld, and T.A. Litovitz, *Absorption and Dispersion of Ultrasonic Waves*, Academic Press, London (1965).
- [15] R. Zwanzig, J. Chem. Phys. **43**, 714 (1965).
- [16] D. Fioretto, G. Carlotti, L. Palmieri, G. Socino, L. Verdini, A. Livi, Phys. Rev. B., **47**, 15286 (1993); D. Fioretto, L. Palmieri, G. Socino, L. Verdini, J. Non-Cryst. Solids 172-174, 1130 (1994); D. Fioretto, L. Palmieri, G. Socino, L. Verdini, Phys. Rev. B **50**, 605 (1994).
- [17] C. Levelut, Y. Scheyer, J. Pelous, and F. Prochazka, J. Non-Cryst. Solids 235-237, 375 (1998); Y. Scheyer, C. Levelut, J. Pelous, and D. Durand, Phys. Rev. B **57**, 11212 (1998).
- [18] D. Fioretto, M. Mattarelli, C. Masciovecchio, G. Monaco, G. Ruocco, and F. Sette, Phys. Rev. B **65**, 224205 (2002); D. Fioretto, C. Masciovecchio, M. Mattarelli, L. Palmieri, G. Ruocco, and F. Sette, Philos. Mag. B **83**, 273, (2002).
- [19] G. Monaco, D. Fioretto, C. Masciovecchio, G. Ruocco, and F. Sette, Phys. Rev. Lett. **82**, 1776 (1999).
- [20] G. Monaco, D. Fioretto, L. Comez, and G. Ruocco, Phys. Rev. E **63** 061502 (2001).
- [21] G. Monaco, S. Caponi, R. Di Leonardo, D. Fioretto, and G. Ruocco, Phys. Rev. E **62**, R7595 (2000).
- [22] S. Mossa, G. Monaco, and G. Ruocco, Europhys. Lett. **60**, 92 (2002)
- [23] R. Piccirelli, and T. Litovitz, J. Acous. Soc. Am. **29**, 1009 (1957).
- [24] R. Meister, C.J. Marhoeffter, R. Sciamanda, L. Cotter, and T. Litovitz, J. Appl. Phys. **31**, 854 (1960).
- [25] Y.H. Jeong, S. Nagel, and S. Bhattacharya, Phys. Rev. A **34**, 602 (1986).
- [26] H. Dux, and Th. Dorfmueller, Chem. Phys. **40**, 219 (1979).
- [27] C. Demoulin, C.J. Montrose, and N. Ostrowsky, Phys. Rev. A **9**, 1740 (1974).
- [28] Y.X. Yan, L.T. Cheng, and K.A Nelson, J. Chem. Phys. **88**, 6477 (1988).
- [29] D.M. Paolucci, and K.A. Nelson, J. Chem. Phys., **112**, 6725 (2000).
- [30] W.T. Grubbs and R. MacPhail, J. Chem. Phys. **100**, 2562 (1994).
- [31] R. Di Leonardo, A. Taschin, R. Torre, M. Sampoli, and G. Ruocco, Phys. Rev. E **67**, R15102 (2003).
- [32] R. Vacher and J. Pelous, J. Chim. Phys. **82**, 311 (1985).
- [33] J. Wuttke et al., Phys. Rev. Lett. **72**, 3052 (1994).
- [34] E. Rössler et al., Phys. Rev. Lett. **72**, 3052 (1994); E. Rössler, A.P. Sokolov, A. Kisliuk, and D. Quitmann Phys. Rev. B **49**, 14967 (1994).
- [35] A.P. Sokolov, W. Steffen, and E. Rössler, Phys. Rev. E **52**, 5105 (1995).
- [36] P. Lunkenheimer, A. Pimenov, M. Dressel, Yu.G. Goncharov, R. Böhmer, and A. Loidl, Phys. Rev. Lett. **77**, 318 (1996).
- [37] U. Schneider, P. Lunkenheimer, R. Brand, and A. Loidl, J. Non-Cryst. Solids **235-237**, 173-179 (1998).
- [38] A. Schönhals, F. Kremer, A. Hofmann, E.W Fischer, and E. Schlosser, Phys. Rev. Lett. **70**, 3459 (1993).
- [39] F. Sette, M. Krisch, C. Masciovecchio, G. Ruocco, and G. Monaco, Science **280**, 1550 (1998).
- [40] C. Masciovecchio, G. Monaco, G. Ruocco, and F. Sette, A. Cunsolo, M. Krisch, A. Mermet, M. Soltwisch, and R. Verbeni, Phys. Rev. Lett. **80**, 544 (1998).
- [41] G. Ruocco, F. Sette, R. Di Leonardo, D. Fioretto, M. Krisch, M. Lorenzen, C. Masciovecchio, G. Monaco, F. Pignon, and T. Scopigno, Phys. Rev. Lett. **83**, 5583 (1999).
- [42] S. Adichtchev, T. Blochowicz, C. Gainaru, V.N. Novikov, E.A. Rössler, and C. Tschirwitz, J. Phys.: Condens. Matter **15**, S835 (2003).
- [43] M. Fuchs, W. Götze, and A. Latz, Chem. Phys. **149**, 185 (1990).
- [44] W. Philippoff, in *Physical Acoustics*, edited by W.P. Mason, Academic Press (1965).
- [45] D. Fioretto, L. Comez, G. Socino, L. Verdini, S. Corezzi, and P.A. Rolla, Phys. Rev. E **59**, 1899 (1999).
- [46] F. Nizzoli and J.R. Sandercock, in *Dynamical Properties of Solids*, edited by G. Horton and A.A. Maradudin, North-Holland, Amsterdam (1990).
- [47] <http://ghost.fisica.unipg.it/>
- [48] <http://www.esrf.fr/>
- [49] L. Comez, D. Fioretto, L. Palmieri, G. Socino, and L. Verdini, 1997 IEEE Ultrasonics Symp. Proc., 731-734 (1997).
- [50] G. Harrison, *The Dynamic Properties of Supercooled Liquids*, Academic Press (1976).
- [51] T. Christensen, and N.B. Olsen, Phys. Rev. B **49**, R15396 (1994).
- [52] L. Comez, D. Fioretto, G. Monaco, and G. Ruocco, J. Non-Cryst. Solids **307-310**, 148 (2002).
- [53] J. Fabian, and P.B. Allen, Phys. Rev. Lett. **82**, 1478 (1999).
- [54] V. Vand, Research, Suppl. I., 44 (1947).
- [55] K. Schröter, and E. Donth, J. Chem. Phys. **113**, 9101 (2000).
- [56] C. Allain, M. Berard, and P. Lallemand, Mol. Phys. **41**, 429 (1980).
- [57] C.P. Lindsey, and G.D. Patterson, J. Chem. Phys. **73**, 3348 (1980).
- [58] N.O. Birge, and S.R. Nagel, Phys. Rev. Lett. **54**, 2674 (1985); N.O. Birge, Phys. Rev. B **34**, 1631 (1986).
- [59] F. Scarponi, L. Comez, D. Fioretto, and L. Palmieri, Philos. Mag. B, submitted.
- [60] T. Franosch, M. Fuchs, W. Götze, M.R. Mayr, and A.P. Singh, Phys. Rev. E **56**, 5659 (1997).